ISSN: 2640-5571

Research Article

Advances in Nanoscience and Nanotechnology

A Theoretical Study of the Energetic Stability and Electronic Structure of Terminated and P-Doped Diamond (100)-2x1 Surfaces

Shuainan Zhao and Karin Larsson*

Uppsala University, Uppsala, Sweden

***Corresponding author**
Karin Larsson, Department of Chemistry-Ångström Laboratory, Uppsala University, Lägerhyddsvägen 1, 751 21, Uppsala, Sweden Phone: +46 18 4713750; Fax: +46 18 513548; E-mail: karin.larsson@kemi.uu.se

Submitted: 14 Nov 2019; **Accepted**: 19 Nov 2019; **Published**: 25 Nov 2019

Abstract

The combined effect of P-doping and surface-termination on the energetics, and especially the electronic structure, of a diamond (100) surface, has in the present study been investigated by using a Density Functional Theory method. The diamond surface was terminated with any of the following species: H, F, OH, O_{bridge} and NH_2. These adsorbates have earlier experimentally been proven crucial for e.g. applications based on surface electrochemistry. The observed results were analysed with the purpose to obtain a deeper knowledge about the atomic-level cause to the observed effects by the P doping and surface termination. The P dopant was found to have a very minor influence on the averaged adsorption energy for the various terminating species (i.e. with less than 0.17 eV). Moreover, the adsorbates were found to reduce the stability of the P-dopant in the diamond lattice. When analysing the results of the calculated partial density of states, the P dopant was found to contribute with band gap states below the conduction band, out of which one is a donor band. In addition, the surfaces with their terminating species will contribute with empty band gap states just below the CBM of the diamond surfaces. Hence, the combination of P doping and surface termination will induce both donor and acceptor states in the diamond surface band gap, which will improve the usefulness of these specific diamond surfaces in various electronic devices. The work function of a diamond surface is one specific properties that will be affected by substitutional doping and surface termination. Within the present study, the terminating species were found to render a strong impact on the surface work function (as compared to a non-terminated diamond (100)-2x1 surface), with calculated work function values that were even further decreased by P-doping.

Keywords: Diamond, P-Doping, Theory, DFT, Surface Termination, Surfaces, Electronic Structure, Energetic Stability.

Introduction

Diamond, as a material, consists only of carbon atoms. It also shows extraordinary properties; it is the hardest known material and is also chemically inert. In addition, it shows quite unique electrochemical properties, such as a large electrochemical potential window, a low dielectric constant, controllable surface termination, and a high breakdown voltage [1]. However, the large band gap (5.4 eV) limits the usage of diamond for electronic devices. Hence, impurities have been introduced into the diamond lattice in order to eliminate this limitation. Impurities within a diamond lattice can dramatically change both the geometrical and electronic properties. The boron atom is one of the most commonly used p-type dopants. B-doped diamond shows quite promising electrochemical properties, e.g. tuneable electronic conductivity (depending on the boron-carrier concentration in the diamond lattice). Hence, boron-doped diamond (BDD) has been widely used for electronic applications. Nitrogen, as an n-type dopant, has also frequently been studied during the last decades [2-5]. However, the deep donor level of nitrogen (1.7 eV below the conduction band) limits the usage of nitrogen-doped diamond as an effective n-type semiconductor. Thus, phosphorous has instead been introduced as a plausible n-type donor in diamond (111) [6]. Kato et al. produced this type of n-type diamond epilayer on (100)-oriented diamond surfaces [7]. Compared to the carbon atom, the phosphorus atom has a larger atomic radius. Hence, the incorporation of P into the diamond lattice is thermodynamically unfavoured. However, the presence of a P-containing precursor in the gas phase has experimentally proved to increase the CVD growth rate [8, 9]. A synthesis method, with an increased incorporation efficiency of P atoms in the diamond lattice, has recently been achieved [10].

Phosphorus, P, is nowadays the only well-established substitutional n-type donor [8]. n-type diamond heavily doped with P atoms, has recently been obtained with low electric resistivity and low incorporation activation energy [11, 12]. This makes phosphorus-doped diamond more promising for device applications, e.g. as an electron source for bipolar devices [13-15], as Schottky barrier diodes, and for thermionic emission applications [16,17]. Surface termination is the general notation when a surface-binding species is used to uphold the cubic structure, or to change the surface properties of diamond. For instance, hydrogen-terminated diamond surfaces have been found to be hydrophobic [18]. An H-terminated P-doped

diamond surface has also been found to show negative electron affinity (NEA) [19]. (NEA means that electrons in the conduction band of diamond easily emit from the surface). Electron emission from the conduction band of H-terminated P-doped homoepitaxial diamond (111) has experimentally been observed [17, 20]. A thermionic energy converter is an example of an application for especially a P-doped diamond. However, a lower work function with a lower resistivity is required in order to use P-doped diamond as a cathode electrode in a thermionic energy converter [17]. Thus, the magnitude of the work function for P-doped diamond is quite crucial for the specific usage in thermionic energy converters, and more generally in potential electronic devices.

The oxygen atom is also one of the most commonly used diamond surface terminators. Oxygen-terminated diamond surfaces do generally show hydrophilic properties, as well as a positive electron affinity [21]. The oxygen-termination can appear as a surface binding OH, O_{bridge}, C_{ontop}, or OOH groups. Different chemical routes are used to link functional groups to these O-group adsorbates. This procedure is usually performed in e.g. electroanalytical applications [22]. Fluorine-termination will, compared to H-termination, result in an even more hydrophobic diamond surface. In addition, F-terminated diamond surfaces exhibit exceptional electrochemical properties, such as a lower electrocatalytic activity, a wide electrochemical potential window and low background current [23, 24]. Nitrogen-terminated diamond surfaces are generally very chemically reactive and are thereby commonly used as an intermediate for further modification of the diamond surface (e.g., as a linker). For instance, a diamond surface that is terminated with amine (NH_2) can be modified to be used as a functionalized surface in biosensors [25].

All these interesting properties of terminated diamond surfaces make it clear that surface termination is crucial for especially those applications for which diamond can function as an electrode material. The relative stability and the electronic structures of the P-doped diamond surfaces, terminated with either H, O-containing groups, F or NH_2, are therefore very important to study from an atomic-level point of view.

Theoretical modelling has during the last decades been proven to become highly efficient and helpful in the interpretation and prediction of experimental results. In the present study, the diamond (100)-2x1 surface was chosen in order to investigate the electronic properties of variously terminated diamond surfaces. The low-index (100) plane is one of the most frequently obtained surface planes in CVD-grown diamond. In addition, the (100) epitaxial layers are generally believed to have a better electronic quality than their surface (111) equivalent [26]. The purpose with the present study has therefore been to theoretically investigate the combined effect by P-doping and surface termination on the energetics, and especially the electronic structure, of the diamond (100) surface. The method used was the Density Functional Theory (DFT) under periodic boundary conditions. In addition, the models in the calculations include H, OH, F, O_{bridge} O_{ontop} and NH_2 as terminating species. (Non-terminated diamond surfaces were used for reference purposes).

Methods and Methodology

All calculations in the present study were performed by using Density Functional Theory (DFT) under periodic boundary conditions [27]. More specifically, an ultra-soft pseudo potential plane-wave approach was used, based on the PBE generalized gradient approximation (GGA) of the exchange-correlation functional [28,29,30]. As compared to the simpler LDA (local density approximation) method, the GGA method usually gives a better overall description of the electronic subsystem. The reason is that LDA, which is based on the known exchange-correlation energy for a uniform electron gas, is inclined to over bind atoms and therefore to overestimate the cohesive energy in the system under investigation. On the contrary, GGA takes into account the gradient of the electron density, which gives a much better energy evaluation [31]. Due to the presence of unpaired electrons in the systems, all of the calculations were based on spin polarized GGA (i.e., GGSA). With a few exceptions, the calculations in the present work were carried out using the Cambridge Sequential Total Energy Package (CASTEP) program from BIOVIA [32].

As a result of chemical vapour deposition (CVD) of diamond thin films, there are usually different low Miller index planes that will dominate on the surface. The (111) and the 2x1-reconstructed (100) surfaces are the most frequently observed ones. The (100)-2x1 surface has in the present investigation been chosen for studying the diamond surface electronic properties and reactivity tendencies (see Fig. 1). In order to properly simulate the reconstruction and relaxation of the diamond surface planes, a relatively large cell dimension had to be chosen; 4×4. In addition, all individual models consisted of more than 320 atoms in the super cell, distributed over 20 carbon layers. This model size has been tested and been found large enough for the present type of study. As will be shown in Section *Electronic structures*, the middle part (covering the 9^{th} to the 12^{th} C layers) of the diamond slab gives a good description of bulk diamond. Moreover, the value of the energy cut off for the plane wave basis set was set to 370.00 eV. In addition, the Monkhorst-Pack scheme was used for the k-point sampling of the Brillouin zone, which generated a uniform mesh of k points in reciprocal space [33]. The 1×1×1 k-point, as well as the cut-off frequency of 370 eV, have earlier been tested and found to be adequate to use for the present system [34, 35]. Both edges (i.e., upper and lower) of the diamond slab was terminated with any of the following species: (a) F, (b) H, (c) OH, (d) O in ketone position (O_{ontop}), and (e) O in ether position (O_{bridge}), and (f) NH_2. In addition, two phosphorous atoms were substitutionally positioned within the second top C layer and the second C layer from the bottom. Hence, both the upper and lower parts of the diamond slab where thereby identical (i.e., with a surface-parallel mirror plane in the middle of the slab). Test-calculations have also been performed in the present study in order to evaluate the effect by the position of P in the lattice. It was found that P in atomic layer 2 will have the largest effect on the electronic structure of the diamond surface. Moreover, a large vacuum distance between the slabs was used (> 10 Å) in order to avoid inter slab interactions [36]. The atoms in the model systems were allowed to freely relax, using the BFGS algorithm (Broyden-Fletcher-Goldfarb-Sharmo) [37].

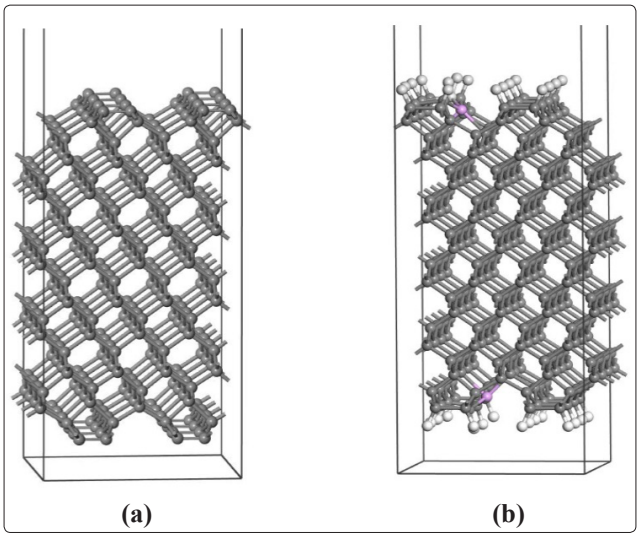

Figure 1: Super cells demonstrating the model of a a) non-terminated, and b) H-terminated P-doped diamond (100)-2x1 surface, respectively. The H, P, and C atoms are shown in white, pink and grey, respectively.

The program Dmol3 from BIOVIA was in the present study used for calculations of the work function [38,39]. The GGA method, based on a PBE non-local functional, was also applied in Dmol3 for single-point energy calculations. All electrons in the systems were included in these calculations. Moreover, the DNP (Double Numerical Potential) atomic orbital basis set was applied for calculations of the surface electronic properties. DNP is a polarized function with an angular momentum that is larger than that of the highest occupied orbital in the free atom. It gives a relatively more reliable description of the electronic structure of the systems under investigation [38].

The work function is defined as "the minimum energy needed to remove an electron from the Fermi level to the vacuum outside the surface". The work function can be calculated by using equation (1).

$$\text{Work function } (\phi) = V(\infty) - E_{Fermi} \quad (1)$$

The potential difference between the electronic potential in a vacuum region far from the surface $V(\infty)$ and the Fermi energy (E_{Fermi}) is the work function for the present systems. Within the present study, the plane-averaged electrostatic potential (V) has been calculated as a function of the position along the z-axis. (The value of the potential in the vacuum region ($V(\infty)$) can be determined for each system by using this approach.) Thus, the work functions of the systems with different surface terminations could here be compared by aligning their respective values of $V(\infty)$.

Structural geometries

The phosphorous atom has a larger atomic radius (110 pm) than the carbon atom (77 pm) [40]. Thus, during the CVD growth process, it is thermodynamically unfavourable to incorporate P into the diamond lattice [41]. The P-induced changes in the diamond structural geometry have therefore been carefully studied in the present investigation. The P-C bond lengths for the various terminated diamond surfaces are shown in Table 1. (The abbreviations that are used in this section are visualised in Figure 2 and presented in Table 1). It should here be mentioned that the geometry optimization of an O_{ontop}-terminated diamond surface resulted in a bulk-like (100)-1x1 surface (shown in Figure 2a). The O species form double bonds with the surface C atoms. Hence, the O species causes a de-reconstruction of the diamond (100)-2x1 surface.

Table 1: The C-P bond lengths for different surface-terminating scenarios; C1: carbon atom in the first layer; C2: carbon atom in the second layer beneath the surface-reconstructed C-C bonds; C3: carbon atom in the second layer between surface-reconstructed C-C bonds. (The abbreviations are shown in Figure 2c)

[Å]	P-C1	P-C2	P-C3
H	1.75	1.95	1.81
OH	1.74	1.86	1.76
F	1.75	1.91	1.78
O_{bridge}	1.77	-	1.95
NH_2	1.74	1.85	1.76
clean	1.68	1.78	1.78
O_{ontop}	1.71	1.75	1.75

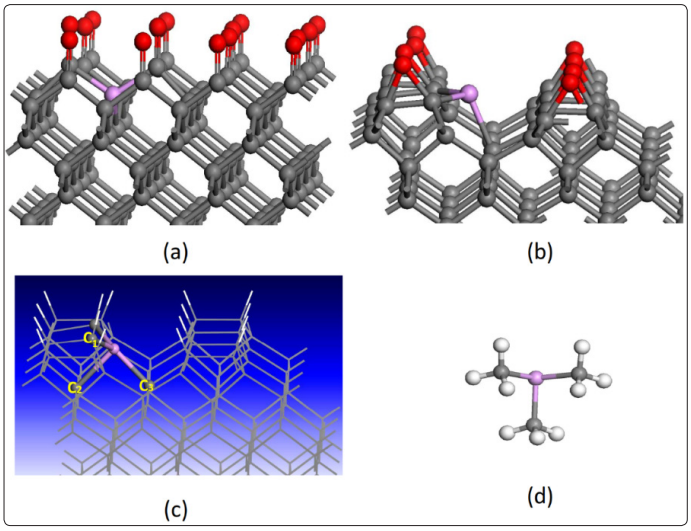

Figure 2: Upper part of the model of a P-doped (a) diamond (100)-1x1 surface with Oontop-termination, (b) (100)-2x1 surface with O_{bridge}-termination, and (c) (100)-2x1 surface with H-termination, respectively. The last model visualizes the binding C atoms (to the P dopant) with the following abbreviations: C1: first-layer carbon; C2: second-layer carbon beneath the surface-reconstructed C-C bond; C3: second-layer carbon in between the surface-reconstructed C-C bonds. (d) shows a model of the $P(CH_3)_3$ molecule

The molecule $P(CH_3)_3$ (see Figure 2d) has been used as a reference compound with the purpose to compare P-C bond lengths. (The P-C bond length in $P(CH_3)_3$ is 1.84 Å). Since the C-C bond length in non-doped diamond is much shorter (1.53 Å), doping by a phosphorous atom will induce bond prolongation. With one exception, P within the second C layer in non-terminated, and variously terminated diamond surfaces, form four P-C bonds. For the O_{bridge}-terminated surface, three of the valence electrons within P prefer to form three bonds with neighbouring carbon atoms. The other two electrons form an electron pair (see Figure 2b). Thus, the P-dopant in the second layer of the O_{bridge}-terminated diamond surface will not offer one

excess electron to form an n-type material. This situation of losing the n-type property will be further discussed in Section *P-induced band gap states*.

For the non-terminated diamond surface, the incorporation of the phosphorous dopant will, generally seen, have the least disturbance effect on the diamond structure (as demonstrated by especially the P-C1 and P-C2 bond lengths in Table 1). As a matter of fact, the P-C1 bond is the shortest (1.68 Å) when compared with the other termination situations. The P-C1 lengths for the other termination situations are 1.75 Å (H-termination), 1.74 Å (OH-termination), 1.75 (F-termination), 1.77 Å (O_{bridge}), 1.74 Å (NH2), and 1.71 Å (O_{ontop}-termination). Hence, all surface-terminating species will result in a lengthening of the P-C1 bond, as compared with the non-terminated situation. Notably, all these bonds are shorter than the P-C bonds in the $P(CH_3)_3$ molecule (1.84 Å).

For all investigated systems, the other two P-C bonds (i.e., P-C2 and P-C3) are longer than the P-C1 bond. As can be seen in Table 1, the P-C2 lengths are 1.95 Å (H-termination), 1.86 Å (OH-termination), 1.91 (F-termination), 1.85 Å (NH_2), 1.78 (non-termination), and 1.75 Å (O_{ontop}-termination). The P-C3 lengths are 1.81 Å (H-termination), 1.76 Å (OH-termination), 1.78 (F-termination), 1.95 Å (Obridge-termination). 1.76 Å (NH2), 1.78 (non-termination), and 1.75 Å (Oontop-termination). For the situation with an Obridge-termination, the P atom will only bind covalently to two C atoms (which will be discussed further below). Moreover, it should here be stressed that there is an appreciable prolongation of the P-C2 bonds (in relation to the P-C1 and P-C3 bonds) for the various surface termination situations. With one exception, these bond lengths are even longer than for the P-C bond in the molecule $P(CH_3)_3$ (1.84 Å). This observation is most probably the result of the excess electron within the P atom, which will be positioned in an anti-bonding state within the P-C2 bond. Thus, the P-C2 bond prolongation indicates a weakening between the P and C2 atom for the situations with H-, OH-, F-, and NH_2-termination). An analysis of the underlying causes to the bond prolongation (and weakening) for specific surface terminations, will be further presented and discussed in Section *Spin density analysis*.

Doping Formation Energy

The solubility of the P element into the diamond (100)-2x1 surface lattices will most probably strongly correlate to both the surface structural geometry (see Section *Structural geometries*) and surface reactivities. It has therefore also been investigated in the present study. The so called doping formation energy has been calculated by using Eq. 2 [42]:

$$\Delta E_{form} = E_{doped\ surface} - E_{nondoped\ surface} + nE_C - nE_P \quad (2)$$

$E_{doped\ surface}$ and $E_{nondoped\ surface}$ are the total energies for a P-doped and non-doped diamond surface, respectively. n is the number of the dopants (there are two P-dopants in the diamond models) and E_c are E_p the total energies for the carbon and phosphorus dopant, respectively. [Here, the doping formation energy ΔE_{form} is defined as the energy needed to induce the P dopant into the non-terminated and differently terminated diamond surfaces]. As can be seen in Table 2, all doping formation energies of the various surface terminating species are positive. Hence, the process of incorporation of the P-dopant is endothermic. It is, though noticeable that the doping formation energy for a non-terminated surface is smaller (5.5 eV) than that of all the terminated surfaces; O_{bridge} (6.8), H (7.3), O_{ontop} (8.1), F (8.1), OH (8.2), and NH_2 (8.2). For the different terminated surfaces, the order of the formation energy is, hence, $O_{bridge} < H < O_{ontop} = F < OH = NH_2$ (see Table 2). It is thereby possible to conclude that the adsorbates will reduce the stability of the P-dopant in the diamond surface.

Table 2: Averaged adsorption energies (eV per adsorbates) for both P-doped and non-doped diamond (100)-2x1 surfaces, in addition to doping formation energies for H-, F-, OH-, O_{ontop}-, O_{bridge}- and NH_2-terminated surfaces

	H	F	OH	O_{bridge}	NH_2	O_{ontop}	Clean
Adsorption Energy (Non-doped)	-4.15	-4.66	-3.95	-5.77	-2.94	-5.50	-
Adsorption Energy (P-doped)	-4.04	-4.50	-3.79	-5.60	-2.77	-5.34	-
Doping formation energy	7.29	8.05	8.16	6.80	8.19	8.05	5.49

As can be seen from Table 1 and 2, the results for the non-terminated diamond surface show a strong correlation between the smallest obtained doping formation energy and the least doping-influence on the structural geometry. Moreover, the smallest formation energy for the various terminated surfaces (i.e., for the O_{bridge}-termination) can be coupled to the situation where P is covalently bonded to three C atoms only. For the other termination situation, there is no obvious correlation between geometrical structure and doping formation energy.

Spin Density Analyses

Spin density calculations give information about differences betweenαand βelectron spin densities (i.e. spin up versus spin down) in the system under investigation. Hence, these calculations can give further information about the effects by P-doping for various diamond surface terminations. Spin density maps for all P-doped systems (i.e., for the different surface terminations), are plotted in Figure 3. These spin density maps make it possible to visualize the electron spin distribution all over the models. As a result, for most of the terminated systems (with an exception for O-termination), the iso surfaces of spin density are concentrated around the P atom and its binding C atoms. Thus, it is possible to conclude that the effects by the P-dopant are quite local for these specific termination situations, and that the unpaired electron within P will partially move from the P-dopant to its binding C atoms. As can be seen in Fig. 3a and 3b, there is no spin density on the P-dopant, or within the P-C bonds, for the P-doped diamond surface with non- or O_{ontop}-termination. The extra electron from P has partially moved up to the surface carbon atoms. And for the O_{ontop}-terminated surface, extra electron density has even moved up to nearby-positioned surface

C atoms, C=O bonds and terminating O atoms, respectively. Thus, there is no observed anti bonding tendency between the P-dopant and its binding C atoms for either the non-terminated or the O_{ontop}-terminated surface. This explains the occurrence of shortened P-C bonds for both specific termination situations, as compared with the other termination conditions (see Table 1). As mentioned above, for the other terminating scenarios (except for the O_{bridge}-terminated surface), the vicinity of the P-dopant shows a strong spin density. It can be seen from Figure 3 c-f that the direction of this spin tendency is toward the position of the smallest steric repulsion with respect to the C atoms. In addition, the extra electron density induced by the P-dopant has also been found to partially transfer to its binding carbon atoms, and thereby to weakening the P-C bonds and cause a bond elongation (see Fig. 1). For the situation with an Obridge-terminated surface, the paired electrons in the P dopant will not cause any spin density on the P atom. However, the C2 atom in the structure that is not binding to any P atom will have one unpaired electron, which can be visualized as a quite strong spin density (see Figure 3g).

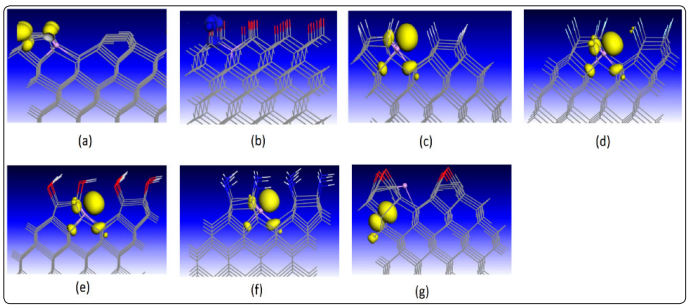

Figure 3: Spin density maps for the supercell models of P-doped diamond (100) surfaces with (a) non-, (b) O_{ontop}-, (c) H-, (d) F-, (e) NH_2-, (f) OH-, and (g) O_{bridge}-termination, respectively. The spin density isosurfaces (of value 0.05/Å), are demonstrated by yellow spheres for all six plots. The H, P, C, O, F and N atoms are shown in light grey, pink, grey, red, green and blue, respectively.

Chemisorption Energies for Attachment of Surface Terminating Species

One way to determine the surface reactivity is to calculate the chemisorption energy for some specific model adsorbates. Within the present investigation, the chemisorption of H, F, O_{bridge}, O_{ontop}, OH and NH_2, respectively, onto P-doped diamond (100)-2x1 surfaces have been studied in order to elucidate the effect of P-doping on the reactivity of this specific surface. Each of these adsorbates is most frequently used in processes like diamond growth, surface functionalization and modifications (as presented in the Introduction). It is therefore of largest interest to investigate more in detail the effect of P doping on the surface reactivity of towards these specific species. The averaged adsorption energies of H, OH, F, O_{bridge}, O_{ontop} and NH_2 have in the present study been calculated by using Eq. 3;

$$E_{ads.avg} = \frac{1}{n}\left[E_{surface} - E_{bare-sur} - nE_n\right] \quad (3)$$

Where $E_{surface}$ is the total energy of the terminated surface, $E_{bare\text{-}sur}$ is the total energy of a clean (i.e., non-terminated) surface, n is the number of a specific terminating species within the super-cell, and is the total energy of the adsorbing gas-phase species (i.e., H, F, O_{bridge}, OH or NH_2). This averaged value will give information about the more global effect by the P dopant (i.e., on the whole surface within the super cell). As can be seen in Table 3, the different numbers are negative, so the adsorption reactions are exothermic. Moreover, the adsorption energy for the P-doped surface is larger than for the non-doped scenario (i.e., less exothermic). Hence, doping with a P element will both induce a geometrical surface disruptor and a decrease in diamond (100)-2x1surface reactivity. It should though be mentioned that the differences in adsorption energies (for all termination types investigated) between the P- and non-doped diamond surfaces are quite small (of less than 0.2 eV). Thus, there is no significant global effect by the P dopant on the adsorption energy for the adsorbates.

Table 3: Presentation of band gap donor and acceptor states for P-doped surface-terminated diamond (100) surfaces. The surfaces are terminated with H, F, NH_2, OH, and O_{bridge}, respectively. All values are given as beneath the CBM for the diamond surface. (The values are given in eV)

	H	F	NH_2	OH	O_{bridge}
Donor level	2.4	2.4	2.3	2.3	4.1
Acceptor levels	1.7,	1.0	1.0	1.0,	2.4,
	1.0,			0.8,	2.3,
	0.3			0.7,	1.0,
				0.6,	0.8,
					0.3

For both the non-doped and P-doped situations, the order of adsorption energy was calculated to be $O_{bridge} < O_{ontop} < F < H < OH < NH_2$ (see Table 2). This order agrees very well with earlier studies for non-, N-, and B-doped diamond (100)-2x1 surfaces [43]. Hence, the O_{bridge}-termination resulted in the strongest adsorption. Furthermore, due to strong steric repulsions between the relatively large OH and NH_2 adsorbates, respectively, these two terminating groups give the smallest adsorption binding conditions. The adsorption energies for all species are; -5.8 (O_{bridge}), -5.5 (O_{ontop}), -4.7 (F), -4.2 (H), -4.0 (OH), and -2.9 (NH_2) eV for non-doped diamond, and -5.6 (Obridge), -5.3 (Oontop), -4.5 (F), -4.0 (H), -3.8 (OH), and -2.8 (NH_2) eV for P-doped diamond. There was no obvious correlation observed between these chemisorption energies and the doping formation energy (see Table 2).

Electronic Structures

General

P-doped diamond is an n-type semiconductor. The phosphorous atom has five valence electrons, which is one more than for the carbon atom. Thus, the excess electron in phosphorous would act as a donor within the diamond lattice. This donor level, which for intrinsic bulk diamond lies around 0.6 eV below the conduction band minimum (CBM), will offer electrons to be available for the excitation to the conduction band [44]. Thus, the P dopant in diamond will decrease the band gap of bulk intrinsic diamond. Moreover, when increasing the P-dopant concentration, the donor band will be broadened. It is assumed that P-doping will show a similar effect on the electronic structure for also the surfaces of diamond. The expected changes in the electronic states, induced by phosphorous doping in an H-terminated diamond (100)-2x1 surface, are schematically shown in Figure 4 (where the valence and the conduction bands are also shown).

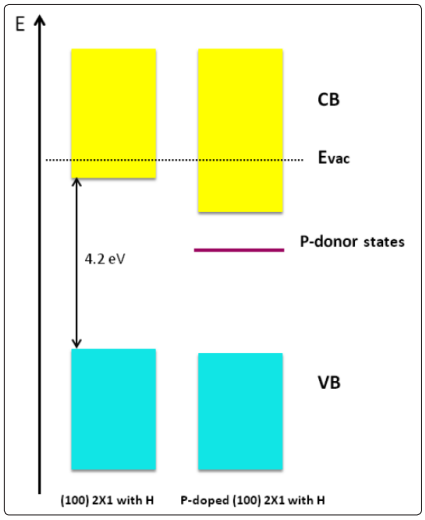

Figure 4: Schematic illustration of the effects of a P-dopant on the H-terminated (100)-2x1 diamond surface. The valence band is represented in blue, the conduction band in yellow, and the phosphorous dopant donor state in red

Figure 5(i) show the Density-Of-States (DOS) for a model describing the non-doped and H-terminated diamond (100)-2x1 surface. [The surface carbon layer (i.e., C1) is included in this C DOS spectra. More over, the Fermi level is aligned to 0 eV]. It should here be mentioned that the DOS spectrum of the bulk-like region of the model indicates the middle part of that specific model (i.e., C atomic layers 10 and 11 (Fig. 1). The DOS spectrum of this middle part is shown in Fig. 5(iii). For comparison, the DOS spectrum of intrinsic bulk diamond is also shown in Fig. 5(iv). When comparing the band gap regions in these figures, the DOS for the bulk-like part of the non-doped diamond surface, with H-termination, is quite similar to the DOS spectra of intrinsic diamond. This is in fact the situation for termination with also the other species; F, OH, NH_2. O_{bridge} and O_{ontop}. Hence, the DOS´s of the middle part of all the models used in the present study have converged to that of bulk diamond, which indicates that these models are sufficently large in order to simulate both the surfaces and their respective bulk part of diamond. This is a result that is very important for the calculations of diamond surface work functions (see Section *Work functions for non-doped and P-doped diamond surfaces*).

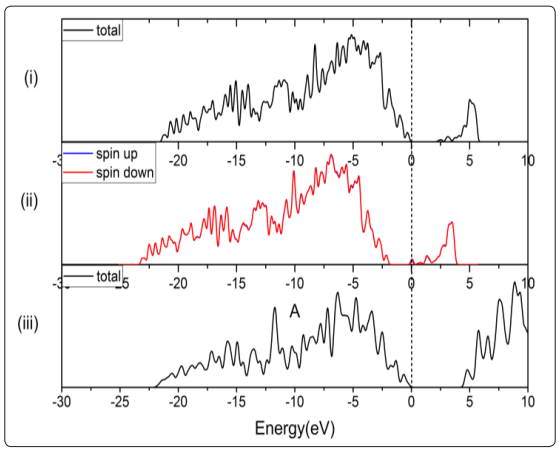

Figure 5: DOS spectra for (i) an H-terminated non-doped diamond (100)-2x1 surface, (ii) an H–terminated P-doped diamond (100)-2x1 surface, and (iii) the bulk of intrinsic diamond. Red line: pDOS of spin up; blue line: pDOS of spin down; black line: total pDOS (i.e. the sum). The spin up and spin down pDOS´s are overlapping in (ii).

As can be seen in Figs. 5 and 6, there are, with only few exceptions, DOS peaks located within the band gap regions for the non- and P-doped diamond (100) surfaces with various surface terminations. Figures 6a shows the DOS spectra for non-doped and F-, OH-, O_{bridge}-, O_{ontop}- and NH_2-terminated diamond (100) surfaces, respectively. The P-doped counterparts are shown in Figures 6b. As was the situation with an H-terminated diamond surface, it is the surface C layer that is included in these DOS spectra. No additional peaks have been observed when including C layers further down in the lattice (i.e., C1 to C9).

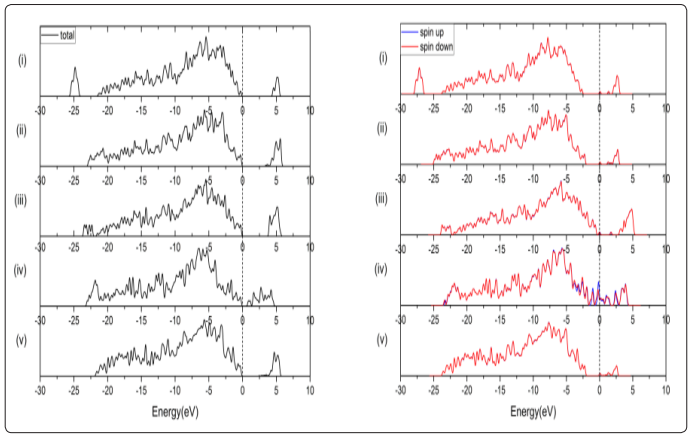

(a) **(b)**

Figure 6: Various carbon partial DOS (i.e., pDOS) spectra for (a) non-doped, and (b) P-doped diamond (100)-2x1 surfaces.[The upper three layers of carbon have been included in these DOS spectra] For both non- and P-doped type, the various pDOS spectra show from top to down: a diamond surface terminated with (i) F, (ii) OH, (iii) Obridge, (iv) Oontop and (v) NH2, respectively. Black line: total DOS (i.e., all atoms).; red line: pDOS of spin up electrons; blue line: pDOS of spin up electrons. The spin up and spin down pDOS´s are overlapping in (b).

It is a well-known fact that the band gap will be underestimated when using DFT calculations, and the present method shows that the calculated band gap for bulk diamond is 4.6 eV, which is to be compared with the experimental value of 5.5 eV (see Fig. 5(iv)). However, it must here be stressed that we are not in this investigation interested in absolute numbers, but instead in trends. Hence, we assume that the in Section *Methods and methodology* presented DFT method is possible to use in the present study.

Band Gap States for Non-Doped Diamond (100) Surfaces

For almost all of the variously terminated non-doped diamond (100) surfaces, band gap states are observed that cannot be found for intrinsic bulk diamond. These additional peaks are most probably induced by the respective surface (i.e. with a specific surface termination). For the F-terminated surface there is no visual evidence for band gap states (see Fig. 6(i). On the other hand, termination with H, OH, NH_2 and O_{bridge} show clear evidences for band gap states. For the H-terminated surface, very weak DOS peaks occur at 2.4, 2.0, 0.9 and 0.6 eV beneath the CBM level (Fig. 5(i)). Moreover, for the OH-terminated surface, one very weak peak occurs at 1.1

eV beneath the CBM level (see Fig. 6(ii)). In addition, the Obridge-terminated surface shows a strong C peak at approximately 0.9 below CBM (Fig. 6(iii). Finally, very weak peaks occur at 2.3, 1.8., 1.4, and 1.0 eV beneath the CBM level for the situation with an NH2-terminated surface (Fig. 6(v)). These band gap states are only distinctly observed when analysing the DOS spectra for the surface C atoms (i.e., for C atoms in carbon layer 1). Moreover, they are are hardly noticed for deeper lying C layers in case of an H-terminating surface, and not observed at all for deeper lying C layers in case of an OH-, NH_2- and Obridge-terminated surface, respectively. This observation is expected since it is preferably the C atomic layer that is mostly affected by the surface-terminating species.

Termination with O_{ontop} species shows another type of scenario. A completely different electronic structure in the region of the band gap can for this termination type be observed. In contradiction to the other surface termination types, the band gap has here decreased to a value of approximately 0.7 eV for C atoms in the closest vicinity to the surface (Fig. 6(iv). In addition, there is no visible band gap state within this narrow band gap. This specific result cannot only be attributed to type of surface-terminating species, but also to the fact that the diamond surface structure is of type (100)-1x1 (in contradiction to the other surface termination types for which the diamond surface is of type (100)-2x1). In short, the band gap structure for a non-doped O_{ontop}-terminated diamond (111) surface gives evidence of a high probability for surface electronic conductivity. This is an observation that also has been made earlier by the present authors [43, 45].

Band Gap States for P-doped Diamond (100) Surfaces

In addition to the band gap states observed for non-doped diamond (100), also P-doped surfaces with their specific terminations will show specific DOS patterns within the diamond band gap. It was found above (Section *Band gap states for non-doped diamond (100) surfaces*) that the band gap states of non-doped diamond surfaces are most probably induced by the respective surface termination. However, those peaks are found to be too weak to be visible in the DOS for the corresponding P-doped surface (see below). Hence, the effect by surface termination on the DOS spectra cannot be observed for the P-doped diamond surfaces.

The DOS spectra for the P-doped and F-, H-, OH-, NH_2-, O_{bridge}- and O_{ontop}-terminated diamond (100) surface, respectively, are shown in Figures 5(ii) and 6b. For the situation with H-, F- or NH_2-termination (Figs. 5(ii), 6b(i), 6b(iii)), all of these scenarios have two large peaks (i.e. band gap states) in common; at 2.4 and 1.0 eV beneath the CBM of the diamond surface. The former peak is filled with electrons, whilst the latter is unfilled. Moreover, all of the C peaks coincide with the P peaks in the band gap. This is most probably due to the hybridization of orbitals between the covalently binding P and C atoms. It is the excess electron in the phosphorous atom that will create the donor level at 2.4 eV beneath the CBM. Since this peak level is the highest occuped level for the P-doped diamond (100) surfaces, the Fermi levels for the variously terminated diamond (100) surfaces have been shifted upwards towards the CBM levels. The lower-lying peak (i.e., 2.4 eV below CBM) is thus positioned at the Fermi levels of the diamond surfaces, and the higher positoned peak at 1.0 eV below CBM is positioned above the Fermi-levels.

There is also one additional (very weak) diamond band gap peak observed for the OH-termination (Fig. 6b(ii)). This peak is empty and located 0.7 eV below CBE. As was the situation for the other band gap states, also this peak can be observed both in the C DOS spectrum and the P DOS spectrum.

The situation with a P-doped and O_{bridge}–terminated diamond surface, was found to be completely different as compared with the H-, F-, NH2-, and OH-terminated surfaces. There was one additional large peak observed just above the VBM level (with 0.8 eV, or 4.1 eV beneath the CBM) (Fig. 6b(iii)). There are, hence, three large peaks positioned within the diamond surface band gap for this specific surface termination, out of which the lowest positioned one (at 0.8 eV above the VBM) is being filled. The underlying cause to the extraordinary position of this peak is the situation with only three covalent P-C bonds for the O_{bridge}-terminated surface (as presented and discussed in Section *Structural geometries*). The reason is most probably that the phosphorous atom in this specific bonding situation will have an electron pair, and as such will lose the capacity to offer one n-type donor electron.

The situation with P-doping and O_{ontop}–termination is completely different as compared with the corresponding non-doped scenario, and with the other termination types. As can be seen in Figure 6b(iv), the diamond surface has now become electronically conducting.

Work Functions for Non-Doped and P-Doped Diamond Surfaces

The combined effect by P-doping and surface-termination on the electronic states within the diamond (100)-2x1 band gap has above been shown to predominantly affect electronic structure and is thereby important for the usage of diamond as a cathode electrode in various electronic devices. More specifically, a thermionic energy converter is an example of an electronic application which requires a lower work function of the electrode material of interest. Thus, the magnitude of the work function for P-doped diamond is quite crucial for the specific usage in thermionic energy converters, and more generally in potential electronic devices. Within the present study, the work functions for non-doped and P-doped diamond surfaces, with different surface terminations, have been calculated by using the $Dmol_3$ program from BIOVIA. As shown in Table 4, the work function was found to be largely affected by both the surface termination and phosphorous doping. As compared to non-terminated and non-doped diamond surfaces, termination of these surfaces will have a strong impact on the surface work function. The H-, NH_2- and OH- terminated surfaces show smaller surface work functions as compared to the non-terminated scenario; 3.62 eV (H), 3.48 eV (NH_2), 4.51 eV (OH) vs. 4.94 eV (Non-termination). The work function for the H-terminated surface (3.62 eV) is in agreement with experimental results (4.20 eV at 50 °C) [46]. Experimental observations have also shown that the H-terminated (100)-(2×1) surface will have a work function that is approximately 1.5 eV lower than the work function for the non-terminated (100)-(2×1) surface [47]. This is most probably due to the smaller electronegativity value of the H atom (2.20), as compared to the C atom (2.55) [40]. The H adsorbates on the diamond surface will thereby form a C-H) dipole. The NH_2 and OH adsorbates, which both have smaller electronegativity than C, will form similar dipoles on the diamond surface. These dipole surfaces have earlier been shown to give an impact on the reduction of the surface work function [48]. In the present investigation, the following order of work function was obtained for H-, NH_2- and OH-termination; OH (4.51eV) > H (3.62 eV) > NH_2 (3.48 eV). NH2-terminated and non-doped diamond (100)-2x1 surfaces will show the smallest surface work function.

For the situation with F- and O-termination, both F atom and O atom have larger electro negativities than C; 3.98, 3.44, and 2.55, respectively. Thus, the calculated work functions for the situations with F-, Obridge-, and Oontop- terminations are 8.02, 6.75, and 8.21 eV (as compared with 4.94 for the non-terminated diamond surface). These values are similar to experimental results that have shown that the work function for an F-terminated diamond (100) surface is 7.24 eV, and for the O-terminated diamond (100) it is 6.4 eV [49]. Hence, out of all termination species used in the present study, surface termination by NH_2 will result in the smallest work function. The order of work functions for all species is; Oontop (8.21 eV) > F (8.02 eV) > Obridge (6.75 eV) > OH (4.51 eV) > H (3.62 eV) > NH_2 (3.48 eV).

Table 4: Presentation of calculated surface-related work functions for non-and P-doped diamond (100) surfaces. These surfaces are either non-terminated or terminated with H, F, NH_2, OH, Obridge and Oontop, respectively. (The numbers are given in eV)

clean	H	F	NH_2	OH	O_{bridge}	O_{ontop}
4.94	3.62	8.02	3.48	4.51	6.75	8.21
4.86	1.40	5.27	1.30	2.22	5.56	7.80

Non-doped diamond (100) surfaces
P-doped diamond (100) surfaces

The effects of a P-dopant on the surface work function are also shown in Table 4. It is quite clear that the surface work function has, for each termination type, been reduced dramatically when substitutionally doping the diamond (100) surface with P. The values for the work functions are 7.80 (O_{ontop}), 5.56 (O_{bridge}), 5.27 (F), 2.22 (OH), 1.40 (H), and 1.30 (NH_2) eV for a P-doped surface, as compared with 8.21 (O_{ontop}), 6.75 (O_{bridge}), 8.02 (F), 4.51 (OH), 3.62 (H), and 3.48 (NH_2) when using a non-doped surface. It has also been experimentally verified that a P-doped diamond surface will have a quite low work function (of 0.9 eV) [50]. The explanation to the fact that P-doped diamond surfaces will have a lower work function is that the phosphorous dopant will, with one exception, offer donor states just below the conduction band minimum of the diamond (100)-2x1 surface. These new states will shift the Fermi level upwards and closer to the vacuum level. Thus, P-doped diamond surfaces show smaller work functions than the non-doped scenarios. For the situation with an O_{bridge}-terminated diamond surface, the P dopant will induce a donor level that is closer to the VBE of the diamond surface. Hence, the P-doped O_{bridge}-terminated diamond surface is also here shown to have one of the largest work functions.

Summary and Conclusion

The main purposes with the present theoretical investigation have been to study the combined effect of P-doping (substitutional) and surface termination on the geometrical stabilisation, surface reactivity and band gap electronic states of the diamond (100) surface. The calculations were based on an ultra-soft pseudo potential DFT method under periodic boundary conditions. The terminating species include H, F, OH, O_{ontop}, O_{bridge} and NH_2.

The P dopant was found to give an impact on the geometrical structural of the diamond surface. With one exception, a marked bond lengthening was observed for one of the four P-C bonds in the respective system with different types of surface termination. This is most probably the result of the extra electron within the P atom, which has been positioned in an anti-bonding state within the specific P-C bond. Thus, the longer bond length indicates a weakening in one of the four P-C bonds. Compared to these bond lengthening situations, there is a different situation for the O_{bridge}-terminated surface were three valence electrons within the phosphorous atom preferred to form three bonds with the neighbouring carbon atoms. Hence, the P atom in the O_{bridge}-terminated surface will only bind to three C atoms, whilst P binds to four neighbouring C atoms for the other surface-termination situations.

Moreover, the process of incorporation of the P-dopant into the diamond lattice was found to be endothermic. Hence, substitutional P-doping is to some extent energetically unfavourable. This result is understandable since quite a large restructuring of the surface geometry was found in the vicinity of the P dopant. The smallest formation energy (i.e., least endothermic process) was found for the situation where P is covalently bonded to three C atoms only (i.e., for the O_{bridge}-termination). For the other termination situations, there was no obvious correlation observed for the geometrical structure and doping formation energy. However, the calculations showed that the adsorbates will reduce the stability of the P-dopant in the diamond surface. For the different terminated surfaces, the order of formation energy became; O_{bridge} (6.8) < H (7.3) < O_{ontop} (8.1) =F (8.1) <OH (8.2) =NH_2(8.2) kJ/mol (i.e. OH- and NH_2-termination results in the most unfavourable geometrical structure). Spin-density calculations were found to strongly support the geometrical findings. There was no observed spin-density (and, hence, anti-bonding tendency) between the P-dopant and its binding C atoms for the O_{ontop}-terminated surface. This explains the occurrence of relative short P-C bonds for this specific termination situation. For the other terminating scenarios (except for O_{bridge}-termination), there were a strong spin density in the vicinity of the P-dopant with a partial transfer of electron density to its binding carbon atoms. This explains the bond lengthening for one of the four P-C bonds in the respective system. For the situation with an O_{bridge}-terminated surface, the paired electrons in the P dopant did not cause any spin density. Instead, the neighbouring C that didn´t bind to the P atom had one unpaired electron which was visualized as a quite strong spin density.

The calculated adhesion energies for the different surface terminating species were found to be useful as a tool for determining the surface reactivity. The P dopant had a very minor influence on the adsorption energies, so the trend in averaged adsorption energy was for both non- and P-doped diamond: O_{bridge} (-5.8, -5.6) <O_{ontop} (-5.5, -5.3) <F (-4.7, -4.5) <H (-4.2, -4.0) <OH (-4.0, -3.8) <NH_2(-2.9, -2.8) kJ/mol. Hence, the most exothermic chemisorption took place for the Obridge species, and the least for the NH_2 species. In addition, this trend in adsorption energy was found to be identical to the order of doping formation energy: O_{bridge} (6.8) <H (7.3) < O_{ontop} (8.1) =F (8.1) <OH (8.2) =NH_2(8.2) kJ/mol. In summary, problem with substitutional doping with P into the diamond (100) surface lattice correlates well with a smaller surface reactivity.

Phosphorous doping and surface termination were shown to induce donor and acceptor states in the bandgap of diamond (100), but the latter to a less extent. For the situation with H-, F-, OH- and NH_2-termination, P doping induced a large donor state and a large acceptor state at approximately 2.4 eV and 1.0 eV, respectively, beneath the CBM of the diamond surface. There is also one additional (very

weak) diamond band gap peak observed for the OH-termination. This peak is empty and located 0.7 eV below CBE. On the contrary, P doping induced three major states for the situation with O_{bridge}-termination; one donor state that was situated 4.1 eV below CBM, and two acceptor states that were situated 2.4 and 1.0 eV beneath CBM. The underlying cause to the extraordinary position of this peak is the situation with only three covalent P-C bonds for this specific termination type. Moreover, the diamond surface has become electronically conducting when using O_{ontop}–termination (i.e. no band gap).

For almost all of the variously terminated non-doped diamond (100) surfaces, band gap states were observed that cannot be found for intrinsic bulk diamond. There were no band gap state observed for the F-terminated surface. For the H-terminated surface, very weak DOS peaks occur at 2.4, 2.0, 0.9 and 0.6 eV beneath the CBM level. Moreover, for the OH-terminated surface, one very weak peak occurs at 1.1 eV beneath the CBM level. In addition, the O_{bridge}-terminated surface shows a strong C peak at approximately 0.9 below CBM. Finally, very weak peaks occur at 2.3, 1.8., 1.4, and 1.0 eV beneath the CBM level for the situation with an NH_2-terminated surface. Termination with O_{ontop} species shows another type of scenario.In contradiction to the other surface termination types, the band gap has here decreased to a value of approximately 0.7 eV. In addition, there is no visible band gap state within this narrow band gap. This specific result cannot only be attributed to type of surface-terminating species, but also to the fact that the diamond surface structure is of type (100)-1x1. In short, the band gap structure for a non-doped O_{ontop}-terminated diamond (111) surface gives evidence of a high probability for surface electronic conductivity.

These results show that the combined effect of P-doping and surface-termination on the electronic states within the diamond (100) band gap will predominantly affect the diamond surface electronic structure and is thereby important for the usage of diamond as a cathode electrode in various electronic devices. More specifically, doping with P will make it possible for the diamond surface to undergo, e.g., photo catalytic excitation from the P donor state to acceptor states in the vicinity of the CBM of diamond (100).

A thermionic energy converter is an example of an electronic application which requires a lower work function of the electrode material of interest. Hence, the effect of surface termination and P-doping has also been studied in the present investigation. It was found that the adsorbates will have a strong effect on the surface work function, as compared to the non-terminated surface. The order of work functions was found to be; Oontop (8.21)>F (8.02) > O_{bridge} (6.75)>OH (4.51) >H(3.62)>NH_2(3.48) eV. Moreover, the surface work functions were further dramatically reduced when substitutionally doping the diamond (100) surface with P, with the resulting order; O_{ontop} (7.80)>Obridge (5.56)>F (5.27)> OH (2.22)>H (1.40)> NH_2(1.30) eV.

Acknowledgement

This project has received funding from the European Union's Horizon 2020 Program under Grant Agreement No. 665085 (DIACAT). The calculations have been performed by using software from BIOVIA.

References

1. Shenai K, Scott RS, Baliga BJ (1989) Optimum semiconductors for high-power electronics. Electron Devices IEEE Transactions 36: 1811-1823.
2. Bhattacharyya S, Auciello S, Birrell J, Carlisle JA, Curtiss LA et al. (2001) Synthesis and characterization of highly-conducting nitrogen-doped ultrananocrystalline diamond films. Appl Phys Lett 79: 1441-1443.
3. Rohrer E, Graeff C, Janssen R, Nebel C, Stutzmann M et al. (1996) Nitrogen-related dopant and defect states in CVD diamond. Phys Rev B 54: 7874-7880.
4. Yu BD, Miyamoto Y, Sugino O (2000) Efficient n-type doping of diamond using surfactant-mediated epitaxial growth. Appl Phys Lett 76: 976-978.
5. Haase A, Peters A, Rosiwal S (2016) Growth and thermoelectric properties of nitrogen-doped diamond/graphite. Dia Relat Mater 63:222-226.
6. Koizumi S, Kamo M, Sato Y, Ozaki H, Inuzuka T (1997) Growth and characterization of phosphorous doped {111} homoepitaxial diamond thin films. Appl Phys Lett 71: 1065-1067.
7. Kato H, Yamasaki S, Okushi H (2005) Growth and characterization of phosphorus-doped diamond using organophosphorus gases. Phys Stat Sol (a) 202: 2122-2128.
8. Frangieh G, Jomard F, Pinault MA (2009) Influence of tertiarybutylphosphine (TBP) addition on the CVD growth of diamond. Phys Stat Sol (a) 206: 1996-1999.
9. Haubner R (2005) Comparison of sulfur, boron, nitrogen and phosphorus additions during low-pressure diamond deposition. Dia Relat Mater 14: 355-363.
10. Ohtani R, Yamamoto T, Janssens SD (2014) Large improvement of phosphorus incorporation efficiency in n-type chemical vapor deposition of diamond. Appl Phys Lett 105: 232106(1-4).
11. Matsumoto T, Kato H, Makino T, Ogura M, Takeuchi D et al. (2014) Carrier transport in homoepitaxial diamond films with heavy phosphorus doping. Jap J Appl Phys 53: 05FP05(1-5)
12. Grotjohn TA. Tran DT, Yaran MK, Demlow SN, Schuelke T (2014) Heavy phosphorus doping by epitaxial growth on the (111) diamond surface. Dia Rel Mater 44: 129-133.
13. Hoshino Y, Kato H, Makino T, Ogura M, Iwasaki T et al. (2012) Electrical properties of lateral p–n junction diodes fabricated by selective growth of n+ diamond. Phys Stat Sol (a) 209: 1761-1764.
14. Makino T, Yoshino K, Sakai N, Uchida K, Koizumi S et al (2011) Enhancement in emission efficiency of diamond deep-ultraviolet light emitting diode. Appl Phys Lett 99: 061110(1-4).
15. Takeuchi D, Makino T, Kato H, Ogura M, Okushi H et al. (2012) High-voltage vacuum switch with a diamond p–i–n diode using negative electron affinity. Jap J Appl Phys 51: 090113(1-7).
16. Suzuki M, Yoshida H, Sakuma N, Ono T, Sakai T et al. (2004) Electrical characterization of phosphorus-doped n-type homoepitaxial diamond layers by Schottky barrier diodes. Appl Phys Lett 13: 2349-2351.
17. Kato H, Takeuchi D, Ogura M, Yamada T, Kataoka M et al. (2015) Heavily phosphorus-doped nano-crystalline diamond electrode for thermionic emission application. Dia Relat Mater 63: 165-168.
18. Marcon L, Spriet C, Coffinier Y, Galopin E, Rosnoblet C et al. (2010) Cell adhesion properties on chemically micropatterned boron-doped diamond surfaces. Langmuir: ACS J Surf Coll 26: 15065-15069.
19. Yamada T, Nebel C, Rezek B, Takeuchi D, Fujimori N et al. (2005) Field emission mechanism of oxidized highly phosphorus-doped homoepitaxial diamond (111). Appl Phys Lett 87: 234107(1-4).

20. Yamada T, Masuzawa T, Mimura H, Okano K (2016) Electron emission from conduction band of heavily phosphorus doped diamond negative electron affinity surface. J Phys D Appl Phys 49: 1-5.
21. De Theije FK, Roy O, van der Laag NJ, van Enckevort WJP (2000) Oxidative etching of diamond. Dia Rel Mater 9: 929-934.
22. Wang M, Simon N, Decorse-Pascanut C, Bouttemy M, Etcheberry A et al. (2009) Comparison of the chemical composition of boron-doped diamond surfaces upon different oxidation processes. Electrochim Acta 54: 5818-5824.
23. Ferro S, De Battisti A (2003) The 5-V window of polarizability of fluorinated diamond electrodes in aqueous solutions. Anal chem 75: 7040-7042.
24. Kondo T, Ito H, Kusakabe K, Ohkawa K, Einaga Y et al. (2007) Plasma etching treatment for surface modification of boron-doped diamond electrodes. Electrochim Acta 52: 3841-3848.
25. Song K-S, Degawa M, Nakamura Y, Kanazawa H, Umezawa H et al. (2004) Surface-modified diamond field-effect transistors for enzyme-immobilized biosensors. Jap J Appl Phys 43: L814-L817.
26. Pinault-Thaury M-A, Stenger I, Jomard F, Chevallier J, Barjon J et al. (2015) Electrical activity of (100) n-type diamond with full donor site incorporation of phosphorus. Phys Stat Solidi (a) 212: 2454-2459.
27. Perdew JP, Burke K, Ernzerhof M (1996) Generalized Gradient Approximation Made Simple. Phys Rev Lett 77: 3865-3868.
28. Petrini D, Larsson K (2008) Origin of the Reactivity on the Nonterminated (100),(110), and (111) Diamond Surfaces: An Electronic Structure DFT Study. J Phys Chem C 112: 14367-14376.
29. Perdew JP, Burke K, Ernzerhof M (1996) Generalized gradient approximation made simple. Phys Rev Lett 77: 3865-3868.
30. Clark SJ (2005) First principles methods using CASTEP. Zeitschrift für Kristallographie 220: 567-570.
31. Monkhorst HJ, Pack JD (1976) Special points for Brillouin-zone integrations. Phys Rev B 13: 5188-5192.
32. Larsson K (2005) Surface properties of diamond under atmospheric conditions: A quantum mechanical approach. New Diamond Front. Carbon Technol 15: 229-245.
33. Segall MD, Shah R, Pickard CJ, Payne, MC (1996) Population analysis of plane-wave electronic structure calculations of bulk materials. Phys Rev B 54: 16317-16320.
34. Parr RG, Yang WT (1984) Density Functional-Approach to the Frontier-Electron Theory of Chemical-Reactivity. J Amer Chem Soc 106: 4049-4050.
35. Yang W, Parr RG, Pucci R (1984) Electron-Density, Kohn-Sham Frontier Orbitals, and Fukui Functions. J Chem Phys 81: 2862-2863.
36. Petrini D, Larsson K (2008) Theoretical study of the thermodynamic and kinetic aspects of terminated (111) diamond surfaces. J Phys Chem C 112: 3018-3026.
37. Lu Y-G, Turner S, Verbeeck J, Janssens S, Haenen K et al. (2013) Local bond length variations in boron-doped nanocrystalline diamond measured by spatially resolved electron energy-loss spectroscopy. Appl Phys Lett 103: 032105(1-5).
38. Delley B (1990) An all-electron numerical method for solving the local density functional for polyatomic molecules. J Chem Phys 92: 508-517.
39. Delley B (2000) From molecules to solids with the DMol3 approach. J Chem Phys 113: 7756-7764.
40. Atkins P (2006) Inorganic chemistry. Oxford University Press.
41. Kajihara SA, Antonelli A, Bernholc J, Car R (1991) Nitrogen and potential n-type dopants in diamond. Phys Rev Lett 66: 2010-2013.
42. Cui XY, Medvedeva JE, Delley B, Freeman AJ, Newman N et al., (2005) Role of embedded clustering in dilute magnetic semiconductors: Cr doped GaN. Phys Rev Lett 95: 256404(1-4).
43. Song Y, Larsson K (2015) A Theoretical Study of the Effect of Dopants on Diamond (100) Surface Stabilization for Different Termination Scenarios. J Phys Chem C 119: 2545-2556.
44. Sque S, Jones R, Briddon P (2006) Structure, electronics, and interaction of hydrogen and oxygen on diamond surfaces. Phys Rev B73: 085313(1-15).
45. Zhao S, Larsson K (2014) Theoretical Study of the Energetic Stability and Geometry of Terminated and B-Doped Diamond (111) Surfaces. J Phys Chem C 118: 1944-1957.
46. Brandes GR, Mills AP (1998) Work function and affinity changes associated with the structure of hydrogen-terminated diamond (100) surfaces. Phys Rev B 58: 4952-4962.
47. Diederich L, Küttel OM, Aebi P, Schlapbach L (1998) Electron affinity and work function of differently oriented and doped diamond surfaces determined by photoelectron spectroscopy. Surf Science 418: 219-239.
48. Zheng WT, Sun CQ, Tay BK (2003) Modulating the work function of carbon by N or O addition and nanotip fabrication. Sol state comm 128: 381-384.
49. Rietwyk KJ, Wong SL, Cao L, O'Donnell KM, Ley L et al. (2013) Work function and electron affinity of the fluorine-terminated (100) diamond surface. Appl Phys Lett 102: 91604(1-4).
50. Koeck FAM, Nemanich RJ, Lazea A (2009) Thermionic electron emission from low work-function phosphorus doped diamond films. Dia Rel Mater 18: 789-791.